Available online at www.sciencedirect.com
SCIENCE DIRECT®
Sensors and Actuators A 109 (2003) 156–164
SENSORS AND ACTUATORS A PHYSICAL
www.elsevier.com/locate/sna

An analytical model for support loss in micromachined beam resonators with in-plane flexural vibrations

Zhili Hao [a,*], Ahmet Erbil [b], Farrokh Ayazi [a]

[a] School of Electrical and Computer Engineering, Georgia Institute of Technology, 777 Atlantic Drive, Atlanta, GA 30332-0250, USA
[b] School of Physics, Georgia Institute of Technology, 837 State Street, Atlanta, GA 30332-0430, USA

Received 18 June 2003; received in revised form 22 September 2003; accepted 24 September 2003

Abstract

This paper presents an analytical model for support loss in clamped–free (C–F) and clamped–clamped (C–C) micromachined beam resonators with in-plane flexural vibrations. In this model, the flexural vibration of a beam resonator is described using the beam theory. An elastic wave excited by the shear stress of the beam resonator and propagating in the support structure is described through the 2D elastic wave theory, with the assumption that the beam thickness (h) is much smaller than the transverse elastic wavelength (λ_T). Through the combination of these two theories and the Fourier transform, closed-form expressions for support loss in C–F and C–C beam resonators are obtained. Specifically, closed-form expression for the support loss in a C–C beam resonator is derived for the first time. The model suggests lower support quality factor ($Q_{support}$) for higher order resonant modes compared to the fundamental mode of a beam resonator. Through comparison with experimental data, the validity of the presented analytical model is demonstrated.

Keywords: Support loss; Beam resonator; Quality factor; Micromachining; Elastic wave; Flexural vibration

1. Introduction

Micromachined beam resonators are of great interest for a wide range of sensing [1–4] and frequency filtering applications [5–8]. For these applications, a key determinant of performance is the mechanical quality factor (Q) of the resonator, which can be expressed as [2]:

$$Q = 2\pi \frac{W}{\Delta W} \tag{1}$$

where ΔW denotes the energy dissipated per cycle of vibration and W denotes the maximum vibration energy stored per cycle. Achieving high quality factor in resonators can improve the sensitivity and resolution of a sensor, or the spectral purity and susceptibility to electronic phase noise of a filter [9,10]. It is therefore desirable to understand and analyze the mechanisms of energy loss, not only for improving the performance of the resonators, but also for establishing their performance limits.

For a beam resonator operating in vacuum, the sources of energy loss mainly consist of support loss, thermoelastic loss and surface loss [4]. Among these losses, the mechanism of thermoelastic loss has been studied extensively [9–13]. Yang et al. [4] and Yasumura et al. [14] have studied surface loss in beam resonators. As far as support loss, some researchers have focused on investigating its mechanism through experimental work [4,14,15]. However, analytical studies on this subject are few. Jimbo and Itao [16] have provided a closed-form expression for the support quality factor of the fundamental mode of a clamped–free beam resonator. Also, Cross and Lifshitz [17] have derived energy transmission formula for the elastic wave in a beam propagating into its support structure based on the two-dimensional elasticity theory. However, their work treated the vibration of a beam as an elastic wave; the support loss was not derived from the viewpoint of the resonant modes of a beam resonator and hence no explicit expressions were provided.

In this paper, we derive an analytical model for calculating the support loss in micromachined clamped–free (C–F) and clamped–clamped (C–C) beam resonators with in-plane flexural vibrations. Based on the physical mechanism of support loss in a beam resonator, some assumptions are made in order to derive closed-form expressions. An analytical model is developed using the well-established theories of resonant beams and 2D elastic waves. Using the Fourier transform, closed-form expressions are derived to estimate support loss of C–F and C–C beam resonators in their

* Corresponding author. Tel.: +1-404-385-0962; fax: +1-404-894-4700.
E-mail address: zhili.hao@ece.gatech.edu (Z. Hao).

0924-4247/$ – see front matter © 2003 Elsevier B.V. All rights reserved.
doi:10.1016/j.sna.2003.09.037

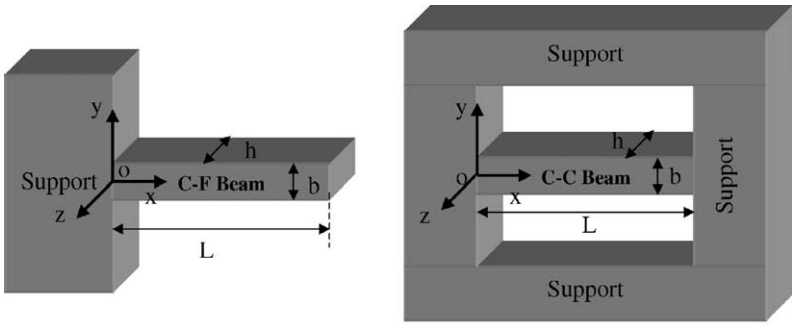

(a) Clamped-free beam (b) Clamped-clamped beam

Fig. 1. Schematic view of beam resonators connected to their supports.

fundamental and higher order modes. Based on this analytical solution, the characteristics of support loss with regard to the design parameters for a beam resonator are discussed. Finally, through comparison with experimental data, the validity of the presented analytical model is demonstrated.

2. Physical mechanisms and modeling assumptions

Fig. 1 shows a schematic view of the two general types of beam resonators, C–F and C–C. The length, width and thickness of the beam resonator are denoted by L, b and h, respectively. The beam resonators operate in their in-plane (x–y plane) flexural vibration modes. Although micromachined beams are generally fabricated with their support regions thicker than the beam resonator itself, this difference in thickness is neglected in our 2D analysis. It is assumed that the dimensions of the supports in the x–y plane are much larger than those of the beam resonators. For simplicity, both the beam resonator and the support regions are assumed to be made of the same isotropic and homogeneous material.

Support loss, also known as clamping loss, is the vibration energy of a resonator dissipated by transmission through its support. During its flexural vibration, a beam resonator will exert both vibrating shear force and moment on its clamped ends. Acting as excitation sources, these vibrating shear force and moment will excite elastic waves propagating into the support. Therefore, the support structure absorbs some of the vibration energy of the beam resonator.

When the elastic wavelength of the propagating wave is much larger than the thickness of the beam (h), the coupling between the resonant modes of a beam resonator and the elastic wave modes in its support is very weak [17]. Hence, the energy transmission from the beam to the support can be treated as perturbation. It is generally assumed that all the vibration energy of a beam resonator that enters its support propagates away to large distances, so that no energy is returned to the beam resonator [9,14,17]. Based on these assumptions, the elastic wave in the support will not have an effect on the resonant modes of the beam. It has been theoretically justified [17] that zero displacement and zero slope of the displacement can be assumed at the clamped ends of a beam resonator. Therefore, the vibration of a beam resonator can be calculated using the well-established beam theory. However, both the vibrating shear force and moment at the clamped ends are non-negligible, which causes energy transmission from the beam into the support, through excitation of elastic waves in the support. The support loss due to the vibrating moment has been theoretically proved to be negligible compared to that incurred by the vibrating shear force [14,17]. Thus, only the support loss due to the vibrating shear stress will be considered in this work, which is formulated as the integral of the product of the shear force and its corresponding displacement in the support over one period.

In order to quantitatively formulate the support loss in a beam resonator in terms of its geometry and resonant mode, it is necessary to assume 2D geometry for the support structure. When the wavelength of the propagating wave is much larger than the beam thickness, there is no z-direction dependency for both the vibration of a beam resonator and the elastic wave in its support. Hence, the difference between the thickness of a beam resonator and its support can be neglected. Furthermore, the supports of a C–F and a C–C beam can be assumed as semi-infinite [17] and infinite thin plates [18], respectively. The behavior of the support can hence be described by the 2D elastic wave theory.

A summary of the assumptions made in our analysis is given below:

(i) The thickness of the beam resonator is much smaller than the wavelength of the elastic wave propagating in its support ($\lambda_T \gg h$).
(ii) The flexural vibration of a beam resonator is described using the ideal beam theory.
(iii) The behavior of the support of a beam resonator is described using the 2D elastic wave theory. The support of C–F and C–C beam resonators are modeled as semi-infinite and infinite thin-plate, respectively, with the same thickness as the beam resonator.
(iv) All the vibration energy of a beam resonator entering the support structure is considered to be lost. It is the vibrating shear force that induces this energy loss.

In the following sections, we briefly review the theories of resonant beams and 2D elastic waves and explain how these two theories can be combined by matching the elastic wave amplitude to the vibrating shear force, to obtain closed-form expressions for support loss in both C–F and C–C beam resonators.

3. Analytical model for a beam resonator

The in-plane flexural vibration of the beam resonator of Fig. 1 can be modeled using the beam theory. The equation for its resonant motion is given by [19]:

$$\frac{\partial^4 y}{\partial x^4} = -\frac{\rho S}{EI}\frac{\partial^2 y}{\partial t^2} \tag{2}$$

where E and ρ denote Young's modulus and density of the beam, I and S are the moment of inertia and cross-section area of the beam, respectively. The coordinates used in this analysis are illustrated in Fig. 1.

When this beam resonator undergoes time-harmonic vibration, we can assume:

$$y(x,t) = Y(x)\,\mathrm{e}^{-\omega t} \tag{3}$$

where ω denotes the angular frequency of the vibration. Substituting (3) into (2), one can obtain:

$$Y = \frac{U}{2}\left\{\cosh\left(\beta\pi\frac{x}{L}\right) - \cos\left(\beta\pi\frac{x}{L}\right) + \chi\left(\sinh\left(\beta\pi\frac{x}{L}\right) - \sin\left(\beta\pi\frac{x}{L}\right)\right)\right\} \tag{4}$$

where β is the mode constant and $U/2$ denotes the vibration amplitude.

χ denotes the mode shape factor and is expressed as:

$$\chi_n = \frac{\sin(\pi\beta_n) - \sinh(\pi\beta_n)}{\cos(\pi\beta_n) + \cosh(\pi\beta_n)} \quad \text{(C–F)} \tag{5}$$

$$\chi_n = \frac{\sin(\pi\beta_n) + \sinh(\pi\beta_n)}{\cos(\pi\beta_n) - \cosh(\pi\beta_n)} \quad \text{(C–C)} \tag{6}$$

where subscript n denotes different resonant mode numbers ($n = 1, 2, 3, \ldots$). Table 1 lists the first 10 mode shape factors and mode constants for both C–F and C–C beam resonators.

The stored flexural vibration energy for each resonant mode of a beam resonator can be expressed as:

$$W_n = \tfrac{1}{8}\rho S L \omega_n^2 U_n^2 \tag{7}$$

where the angular frequency, ω_n, of the nth resonant mode of a beam resonator is [19]:

$$\omega_n = \frac{\pi^2\beta_n^2}{L^2}\sqrt{\frac{EI}{\rho S}} \tag{8}$$

It should be noted that Eqs. (7) and (8) are applicable to both C–F and C–C beam resonators, with different mode-related constant values listed in Table 1.

Through its clamped end, a beam resonator exerts a vibrating shear force Γ_n on its support over the region $x = 0, |y| < b/2$ for a C–F beam, and $x = 0, L, |y| < b/2$ for a C–C beam, respectively:

$$\Gamma_n = EIU_n\left\{\frac{\pi\beta_n}{L}\right\}^3 \chi_n \tag{9}$$

This shear force is assumed to be uniformly distributed across the clamped end, acting as a source to excite elastic waves propagating into the support. Hence, the excitation stress source can be expressed as:

$$\begin{cases} \tau_n = \left|\dfrac{\Gamma_n}{b\cdot h}\right|, & \text{for } |y| \le b/2 \\ 0, & \text{for } |y| > b/2 \\ \sigma_n = 0 \end{cases} \tag{10}$$

where τ_n and σ_n denote the shear and normal stress of the nth resonant mode, respectively. It is the normal stress that contributes to the vibrating moment during the vibration of a beam resonator. Since the support loss caused by the vibrating moment is negligible (as mentioned previously), the normal stress is set to zero.

4. Analytical model for the support structure of a beam resonator

4.1. 2D in-plane elastic waves in a thin-plate

The flexural vibration of a beam resonator excites an elastic wave propagating in its support with in-plane

Table 1
The mode shape factors (χ) and mode constants (β) for C–F and C–C beam resonators

	Mode number									
	1	2	3	4	5	6	7	8	9	10
C–F beam										
β	0.597	1.494	2.5	3.5	4.5	5.5	6.5	7.5	8.5	9.5
χ	−0.734	−1.019	−0.999	−1	−1	−1	−1	−1	−1	−1
C–C beam										
β	1.5056	2.4997	3.5	4.5	5.5	6.5	7.5	8.5	9.5	10.5
χ	−0.983	−1.001	−1	−1	−1	−1	−1	−1	−1	−1

displacement. When the beam thickness is much less than the elastic wavelength, this wave can be treated as a 2D elastic wave described by [18]:

$$\frac{\partial^2 u_x}{\partial t^2} = c_{\mathrm{L}}^2 \frac{\partial^2 u_x}{\partial x^2} + c_{\mathrm{T}}^2 \frac{\partial^2 u_x}{\partial y^2} + (c_{\mathrm{L}}^2 - c_{\mathrm{T}}^2) \frac{\partial^2 u_y}{\partial x \partial y} \tag{11}$$

$$\frac{\partial^2 u_y}{\partial t^2} = c_{\mathrm{L}}^2 \frac{\partial^2 u_y}{\partial y^2} + c_{\mathrm{T}}^2 \frac{\partial^2 u_y}{\partial x^2} + (c_{\mathrm{L}}^2 - c_{\mathrm{T}}^2) \frac{\partial^2 u_x}{\partial x \partial y} \tag{12}$$

where u_x and u_y are the displacements along the x- and y-axis, respectively. The propagation velocities for longitudinal (c_{L}) and transverse waves (c_{T}) are given by:

$$c_{\mathrm{L}}^2 = \frac{E}{\rho(1-\upsilon^2)} \tag{13}$$

$$c_{\mathrm{T}}^2 = \frac{E}{2\rho\,(1+\upsilon)} \tag{14}$$

The Poisson's ratio of the thin-plate is denoted by υ. The longitudinal wavelength and the transverse wavelength can be expressed as:

$$\lambda_{\mathrm{L,T}} = \frac{C_{\mathrm{L,T}}}{f} \tag{15}$$

where f is the frequency of the excitation source, which is same as the resonant frequency of the beam resonator.

The longitudinal propagation velocity is larger than the transverse velocity, since υ is always less than 0.5. Therefore, the longitudinal wavelength is larger than the transverse wavelength, and hence the condition for the validity of the 2D thin-plate analysis for the support region can be mathematically expressed as:

$$\frac{\lambda_{\mathrm{T}}}{h} \gg 1 \tag{16}$$

By assuming $u_x = u\,\mathrm{e}^{\mathrm{i}\omega t}$, $u_y = v\,\mathrm{e}^{\mathrm{i}\omega t}$, and using the following definitions:

$$\Delta = \frac{\partial u}{\partial x} + \frac{\partial v}{\partial y} \tag{17}$$

$$\Omega = \frac{\partial u}{\partial y} - \frac{\partial v}{\partial x} \tag{18}$$

Eqs. (11) and (12) can be rewritten as:

$$-\omega^2 u = c_{\mathrm{L}}^2 \frac{\partial \Delta}{\partial x} + c_{\mathrm{T}}^2 \frac{\partial \Omega}{\partial y} \tag{19}$$

$$-\omega^2 v = c_{\mathrm{L}}^2 \frac{\partial \Delta}{\partial y} - c_{\mathrm{T}}^2 \frac{\partial \Omega}{\partial x} \tag{20}$$

The above two equations can be further reorganized as:

$$c_{\mathrm{L}}^2 \left(\frac{\partial^2 \Delta}{\partial x^2} + \frac{\partial^2 \Delta}{\partial y^2} \right) + \omega^2 \Delta = 0 \tag{21}$$

$$c_{\mathrm{T}}^2 \left(\frac{\partial^2 \Omega}{\partial x^2} + \frac{\partial^2 \Omega}{\partial y^2} \right) + \omega^2 \Omega = 0 \tag{22}$$

The shear stress toward the y-axis and the normal stress toward the x-axis are given by [18]:

$$\tau = \frac{E}{1+\upsilon} \left(\frac{\partial u}{\partial y} + \frac{\partial v}{\partial x} \right) \tag{23}$$

$$\sigma = \frac{E}{1-\upsilon^2} \left(\frac{\partial u}{\partial x} + \upsilon \frac{\partial v}{\partial y} \right) \tag{24}$$

respectively, which is also rewritten as:

$$\frac{\omega^2}{\rho c_{\mathrm{T}}^4} \tau = \left[\frac{\partial^2 \Omega}{\partial x^2} - \frac{\partial^2 \Omega}{\partial y^2 \Omega} \right] - 2 \frac{c_{\mathrm{L}}^2}{c_{\mathrm{L}}^2} \frac{\partial^2 \Delta}{\partial x \partial y} \tag{25}$$

$$\frac{\omega^2}{\rho c_{\mathrm{T}}^4} \sigma = -2 \frac{\partial^2 \Omega}{\partial x \partial y} - \frac{c_{\mathrm{L}}^4}{c_{\mathrm{T}}^4} \frac{\partial^2 \Delta}{\partial x^2} + \left(2 \frac{c_{\mathrm{L}}^2}{c_{\mathrm{T}}^2} - \frac{c_{\mathrm{L}}^4}{c_{\mathrm{T}}^4} \right) \frac{\partial^2 \Delta}{\partial y^2} \tag{26}$$

4.2. Fourier transform of the 2D in-plane elastic waves in a thin-plate

As mentioned in Section 2, support loss is related to the displacement in the support along the direction of the shear stress. This displacement, v, has been implicitly expressed by the 2D in-plane elastic wave theory in the above subsection. In order to obtain an explicit expression from this theory, we apply the Fourier transform to Eqs. (19)–(22), (25) and (26) [20]. The following equations are obtained:

$$-\omega^2 u_{\mathrm{F}} = c_{\mathrm{L}}^2 \frac{\mathrm{d}\Delta_{\mathrm{F}}}{\mathrm{d}x} - i\xi c_{\mathrm{T}}^2 \Omega_{\mathrm{F}} \tag{27}$$

$$\omega^2 v_{\mathrm{F}} = c_{\mathrm{L}}^2 i\xi \Delta_{\mathrm{F}} + c_{\mathrm{T}}^2 \frac{\mathrm{d}\Omega_{\mathrm{F}}}{\mathrm{d}x} \tag{28}$$

$$\frac{\mathrm{d}^2 \Delta_{\mathrm{F}}}{\mathrm{d}x^2} - \left(\xi^2 - \frac{\omega^2}{c_{\mathrm{L}}^2} \right) \Delta_{\mathrm{F}} = 0 \tag{29}$$

$$\frac{\mathrm{d}^2 \Omega_{\mathrm{F}}}{\mathrm{d}x^2} - \left(\xi^2 - \frac{\omega^2}{c_{\mathrm{T}}^2} \right) \Omega_{\mathrm{F}} = 0 \tag{30}$$

$$\frac{\omega^2}{\rho c_{\mathrm{T}}^4} \tau_{\mathrm{F}} = \left[\frac{\mathrm{d}^2 \Omega_{\mathrm{F}}}{\mathrm{d}x^2} + \xi^2 \Omega_{\mathrm{F}} \right] + 2i\xi \frac{c_{\mathrm{L}}^2}{c_{\mathrm{T}}^2} \frac{\mathrm{d}\Delta_{\mathrm{F}}}{\mathrm{d}x} \tag{31}$$

$$\frac{\omega^2}{\rho c_{\mathrm{T}}^4} \sigma_{\mathrm{F}} = 2i\xi \frac{\mathrm{d}\Omega_{\mathrm{F}}}{\mathrm{d}x} - \frac{c_{\mathrm{L}}^4}{c_{\mathrm{T}}^4} \frac{\mathrm{d}^2 \Delta_{\mathrm{F}}}{\mathrm{d}x^2} - \left(2 \frac{c_{\mathrm{L}}^2}{c_{\mathrm{T}}^2} - \frac{c_{\mathrm{L}}^4}{c_{\mathrm{T}}^4} \right) \xi^2 \mathrm{d}\Delta_{\mathrm{F}} \tag{32}$$

where subscript F denotes the Fourier transform and ξ is the variable of this transform.

The solutions for Eqs. (29) and (30) can be expressed as:

$$\Delta_{\mathrm{F}} = A\,\mathrm{e}^{\sqrt[x]{\xi^2 - (\omega/c_{\mathrm{L}})^{2\cdot x}}} \tag{33}$$

$$\Omega_{\mathrm{F}} = B\,\mathrm{e}^{\sqrt[x]{\xi^2 - (\omega/c_{\mathrm{T}})^{2\cdot x}}} \tag{34}$$

respectively, when $x \leq 0$. A and B are constants related to the amplitude of the elastic wave and can be specified by Eqs. (31) and (32) with the appropriate excitation stress

source from a beam resonator. Finally, the displacement under the stress source can be found by substituting the solutions (33) and (34) into Eq. (28).

5. Closed-form expressions for support loss in micromachined beam resonators

5.1. Clamped–free beam resonators

The support of a C–F beam resonator is modeled as a semi-infinite thin plate of thickness h in the x–y plane as shown in Fig. 2, where σ_n and τ_n are the normal and shear stress of the nth in-plane flexural resonant mode of the beam resonator, respectively. The stress sources, introduced in (10), are transformed into:

$$\begin{cases} \tau_{\mathrm{F}} = \dfrac{2\tau_n \sin(\xi(b/2))}{\xi}, & x = 0 \\ \sigma_{\mathrm{F}} = 0, & x = 0 \end{cases} \tag{35}$$

By combining (28) to (35) and applying the inverse Fourier transform, the average displacement along the y-axis and over the source region can be expressed as:

$$v_{(x=0)} = \frac{4b\tau_n}{\pi E}\frac{1+\upsilon}{1-\upsilon}\Psi \tag{36}$$

where

$$\Psi = \int_0^\infty \frac{\sqrt{\zeta^2 - (c_{\mathrm{L}}/c_{\mathrm{T}})^2}}{\left\{2\zeta^2 - (c_{\mathrm{L}}/c_{\mathrm{T}})^2\right\}^2 - 4\zeta^2 \cdot \sqrt{\zeta^2 - (c_{\mathrm{L}}/c_{\mathrm{T}})^2} \cdot \sqrt{\zeta^2 - 1}}\,\mathrm{d}\zeta \tag{37}$$

and $\zeta = \xi c_{\mathrm{L}}/\omega$. The imaginary part of the integral of (37), which will contribute to support loss, can be numerically calculated to be 0.336 (assuming $\upsilon = 0.28$).

After the displacement incurred by the shear stress over the source region is determined, the amount of energy loss per cycle from the support of a beam resonator can be explicitly calculated as:

$$\Delta W = \pi \Gamma_n v_{(x=0)} \tag{38}$$

where the coefficient π is due to the time-harmonic nature of the shear force and its corresponding displacement.

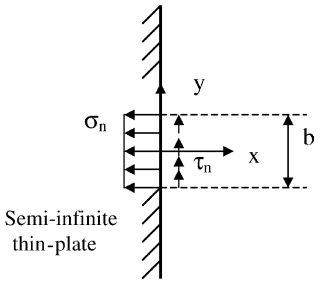

Fig. 2. A semi-infinite thin-plate with excitation source from a C–F beam resonator.

By combining Eqs. (1), (7) to (10), (36), and (38), the support quality factor of a C–F beam resonator can be expressed as:

$$Q_{\mathrm{C-F}(n)} = \left[\frac{0.24(1-\upsilon)}{(1+\upsilon)\Psi}\right]\frac{1}{(\beta_n\chi_n)^2}\left[\frac{L}{b}\right]^3 \tag{39}$$

Comparing Eq. (39) with the results obtained by Jimbo and Itao [16], the $Q_{\mathrm{C-F}}$ value predicted by Eq. (39) is 4% smaller than the result of Jimbo and Itao, which is based on the assumption of the support as a semi-infinite solid (assuming $\upsilon = 0.25$). Since the assumption of semi-infinite thin-plate versus semi-infinite solid incurs very small variation of the propagation velocities of the longitudinal waves in the support, the difference between the predictions of these two models is trivial. However, for a beam resonator with a large ratio of λ_{T}/h, it is more practical to assume the support as a semi-infinite thin-plate than a semi-infinite solid.

5.2. Clamped–clamped beam resonators

For a C–C beam resonator, the support is modeled as an infinite thin-plate of thickness h in the x–y plane as shown in Fig. 3, and the stress sources are distributed over two regions at $x = 0$, $|y| < b/2$ and $x = L$, $|y| < b/2$:

$$\begin{cases} \tau_{\mathrm{F}} = \dfrac{2\tau_n \cdot \sin(\xi \cdot b/2)}{\xi}, & x = 0, L \\ \sigma_{\mathrm{F}} = 0, & x = 0, L \end{cases} \tag{40}$$

By combining (28)–(34) and (40) and applying the inverse Fourier transform, the average displacement along y-axis over the source region $x = 0$, $|y| \le b/2$, can be expressed as:

$$v_{x=0} = \frac{b \cdot \tau_n}{16 \cdot E} \cdot (3-\upsilon) \cdot (1+\upsilon) + \frac{b \cdot \tau_n}{4 \cdot \pi \cdot E} \cdot \Pi \tag{41}$$

where

$$\Pi = (1-\upsilon^2)\int_0^1 \frac{\xi^2}{\sqrt{1-\xi^2}} \cos\left(\sqrt{1-\xi^2}\frac{\omega L}{c_{\mathrm{L}}}\right)\mathrm{d}\xi + 2(1+\upsilon)\int_0^1 \sqrt{1-\xi^2}\cos\left(\sqrt{1-\xi^2}\frac{\omega L}{c_{\mathrm{T}}}\right)\mathrm{d}\xi \tag{42}$$

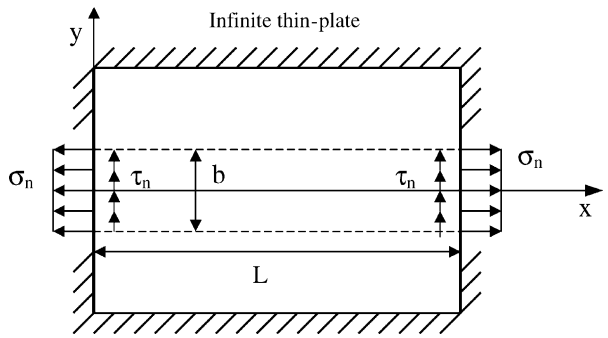

Fig. 3. An infinite thin-plate with excitation source from a C–C beam resonator.

It should be noted that the displacement expressed by Eq. (41) is only the imaginary part of the average displacement. The first and second terms in Eq. (41) are incurred by the stress sources at $x = 0$ and L, respectively. The second term is always smaller than the first term, which can be explained by the fact that the stress source at $x = 0$ induces larger displacement over its own adjacent region.

Due to the symmetry of the C–C beam around $x = L/2$, the displacement along y-axis over the source region $x = L, |y| \leq b/2$ can also be calculated using Eq. (41). Thus, the support quality factor of a C–C beam resonator can be expressed as:

$$Q_{\mathrm{C\text{–}C}(n)} = \left\{ \frac{2.43}{(3-\upsilon)(1+\upsilon)} + \frac{1.91}{\Pi} \right\} \frac{1}{(\beta_n \chi_n)^2} \left[\frac{L}{b} \right]^3 \quad (43)$$

When the elastic wavelength is very large compared to the beam length (L), the second term in the square braces is approximately equal to the first term. It is worth mentioning that the values of β and χ are mode-related and different for Eqs. (39) and (43), since they represent different types of beam resonators.

5.3. Discussions

The analytical model for the support loss derived in this paper provides insight into the design of microresonators, which are summarized as below:

(i) *Dimensional dependency:* The support quality factor (Q_{support}) is proportional to the cubic power of the ratio of the beam length to the beam width $(L/b)^3$, independent of the beam thickness (h).

(ii) *Material properties:* While the support quality factor of a beam resonator is independent of the Young's modulus of the resonator's material, it is dependent on the Poisson's ratio of the resonator's material. The influence of the Poisson's ratio is introduced by the transition of 1D vibration in the beam resonator into 2D elastic wave propagation in the support structure.

(iii) *Vibration amplitude:* The support quality factor has no dependency on the vibration amplitude, as long as the vibration amplitude of the beam resonator is kept in the linear range.

(iv) *Mode order:* The support quality factor of a micromachined C–F or C–C beam resonator decreases as its mode order increases. Illustrated in Fig. 4 are the plots of the coefficients of $(L/b)^3$ in Eqs. (39) and (43) versus resonant mode orders, assuming a Poisson's ratio of 0.28. The difference between the first and second terms in Eq. (43) is neglected in this figure.

6. Experimental verification

6.1. Thermoelastic damping and surface loss related quality factors

For a beam resonator operating in vacuum, the overall quality factor (Q) can be expressed as:

$$\frac{1}{Q} = \frac{1}{Q_{\mathrm{support}}} + \frac{1}{Q_{\mathrm{TED}}} + \frac{1}{Q_{\mathrm{surface}}} \quad (44)$$

where Q_{support}, Q_{TED}, and Q_{surface} denote the quality factors due to the three energy loss mechanisms of support loss, thermoelastic damping, and surface loss, respectively. The losses due to any other sources are assumed negligible in this work. In order to experimentally verify the analytical

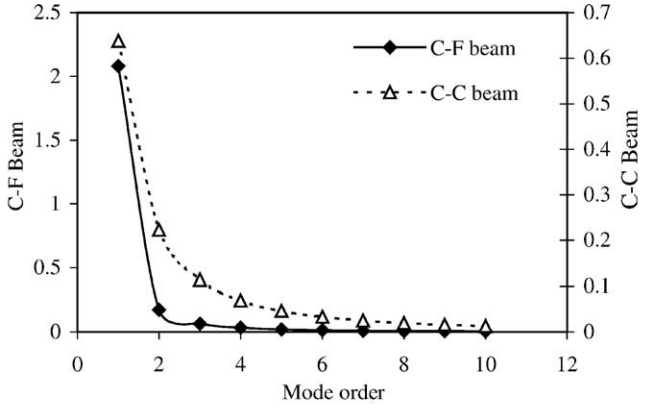

Mode order	1	2	3	4	5	6	7	8	9	10
C-F beam	2.081	0.173	0.064	0.033	0.020	0.013	0.009	0.007	0.006	0.004
C-C Beam	0.638	0.223	0.114	0.069	0.046	0.033	0.025	0.019	0.015	0.013

Fig. 4. The coefficients $\{0.24(1-\upsilon)/(1+\upsilon)\Psi\}\{1/(\beta_n\chi_n)^2\}$ and $\{2 \times 2.43/(3-\upsilon)(1+\upsilon)\}\{1/(\beta_n\chi_n)^2\}$ of the predicted support quality factors of a C–F and a C–C beam resonator.

Table 2
Material properties of highly-doped single-crystal silicon

Property	Symbol	Value
Density (kg/m^3)	ρ	2330
Young's modulus for Si[1 0 0] (Pa)	E	1.3×10^{11}
Poisson's ratio for Si[100]	υ	0.28
Thermal expansion coefficient (K)	α_T	2.6×10^{-6}
Specific heat (J/(K m^3))	C_p	1.63×10^{6}
Thermal conductivity (W/(m K))	κ	90
Environmental temperature (K)	T_0	300

model for support loss derived in this paper, both Q_{TED} and $Q_{surface}$ components of the measured overall quality factor need to be quantified.

The Q_{TED} can be expressed as [12]:

$$\frac{1}{Q_{TED}} = \frac{E\cdot\alpha_{T^2}.T_0}{C_{p\cdot}\rho}\cdot\left\{\frac{6}{\varsigma^2}-\frac{6}{\varsigma^3}\cdot\frac{\sinh(\varsigma)+\sin(\varsigma)}{\cosh(\varsigma)+\cos(\varsigma)}\right\} \quad (45)$$

where α_T and C_p denote thermal expansion coefficient and specific heat at constant pressure of the material used for the beam, respectively; T_0 is the environmental temperature; ς is expressed as:

$$\varsigma = b\sqrt{\frac{\omega\rho C_p}{2\kappa}} \quad (46)$$

where κ denotes thermal conductivity of the beam material and ω denotes the angular frequency of the beam resonator.

Yang et al. [4] suggests the following expression for the $Q_{surface}$:

$$Q_{surface} = \frac{bh}{3b+h}\frac{E}{2E_{ds}\delta} \quad (47)$$

where δ denotes the characterized thickness of the surface layer and E_{ds} is a constant related to the surface stress. If the C–F beam and C–C beam resonators are fabricated using the same process, we can argue that δ should be the same for both C–F and C–C while the E_{ds} of a C–F beam resonator is smaller than that of a C–C beam resonator, in that only one end of a C–F beam is constrained. Since it is very difficult to characterize the values of δ and E_{ds}, we will choose the best-fit values of $E_{ds}\delta$ to minimize the error between the model and the experimental data in the following subsection.

6.2. Comparison with experimental data

In order to demonstrate its validity, this analytical model is compared with the experimental data detailed in the literature [13]. The C–F and C–C beam resonators in [13] were made of highly-doped single-crystal silicon, which is an anisotropic material. The model developed in this paper is for isotropic material. However, since the boundary planes of the fabricated beam resonators of [13] are all [1 0 0], we can use the material properties of single crystal silicon along the ⟨1 0 0⟩ orientation for the model [21]. The material properties used in this work are listed in Table 2 [13]. The beam thickness is 20 μm for all the measured silicon resonators. Due to its critical role in estimating the support loss, the "mask-drawn" beam widths listed in [13] have been slightly modified in our calculations to match the "measured" resonant frequencies of the resonators and account for lithography and fabrication error. Only the data points that satisfy the $\lambda_T/h \gg 1$ condition (2D analysis) were considered.

Table 3 lists the measured quality factors ($Q_{measured}$) and calculated support quality factors ($Q_{support}$) of the fundamental mode of different sizes of single crystal silicon C–C beam resonators without surface treatment. The $Q_{analytical}$ is the overall quality factor calculated using Eq. (44). Also listed in Table 3 are the Q_{TED} and the $Q_{surface}$ with $E_{ds}\delta$ equal to 1.38, calculated from Eq. (45) and (47), respectively. Table 4 compares the $Q_{measured}$ with the calculated quality factors of the fundamental mode of different sizes of C–C beam resonators *with surface treatment* (to reduce surface roughness, the beams were oxidized and the oxide was subsequently removed). Since our calculation shows that the surface treatment makes $Q_{surface}$ negligible compared to Q_{TED} and $Q_{support}$, the $Q_{surface}$ is not listed in this table. The calculated and measured quality factors are in good agreement for both *with* and *without* surface treatment. Especially, for C–C beam resonators *with surface treatment*, errors introduced by surface loss are greatly alleviated and hence the comparison between the developed model and the experimental data is much more reliable.

Table 5 compares the $Q_{measured}$ and calculated $Q_{support}$ of the fundamental mode of different sizes of single crystal silicon C–F beam resonators without surface treatment. It is found that $E_{ds}\delta = 0.81$ works well for the C–F beam resonators. As expected, the value of $E_{ds}\delta$ for a C–F beam resonator is smaller than that of a C–C beam resonator, and the calculated and measured values of quality factor are agreeable.

The comparison between the $Q_{measured}$ and calculated $Q_{support}$ for the third resonant mode of different size single

Table 3
Comparison between measured quality factors and calculated support quality factors of the fundamental mode of different sizes of single crystal silicon C–C beam resonators without surface treatment (the first data point was taken from [22], which used the same fabrication technology as [13])

Length (μm)	Width (μm)	Measured frequency (kHz)	λ_T/h	$Q_{support}$	Q_{TED}	$Q_{surface}$	$Q_{analytical}$	$Q_{measured}$
900	7.9	74.8	3120	248470	116590	173760	54476	53600
700	5.15	80.3	2907	421980	254010	139464	74201	74000
500	3.8	117	1995	382800	322520	116178	69831	67000
300	3.4	288.4	809	115440	162280	108079	41533	43000

Table 4
Comparison between measured quality factor and calculated support quality factor of the fundamental mode of different sizes of single crystal silicon C–C beam resonators with surface treatment

Length (μm)	Width (μm)	Measured frequency (kHz)	λ_T/h	$Q_{support}$	Q_{TED}	$Q_{analytical}$	$Q_{measured}$
500	5.35	164.5	1419	130280	115870	61327	60400
500	6.45	198	1179	74345	66523	35108	35000
500	7.1	217	1076	56933	51264	26975	27000
700	8	125.5	1860	106920	68302	41678	39400

Table 5
Comparison between measured quality factor and calculated support loss quality factor of the fundamental mode of different sizes of single crystal silicon C–F beam resonators without surface treatment

Length (μm)	Width (μm)	Measured frequency (kHz)	λ_T/h	$Q_{support}$	Q_{TED}	$Q_{surface}$	$Q_{analytical}$	$Q_{measured}$
700	6.45	15.94	14642	2662600	821910	262262	185006	173800
500	4	19	12284	4068400	1758100	200000	171981	178000
500	5	24.59	9492	2083000	900180	228571	167617	157400
500	6.2	30.14	7744	1092500	472190	256995	144420	154800

Table 6
Comparison between measured quality factor and calculated support quality factor of the 3rd resonant mode of different sizes of single crystal silicon C–C beam resonators with surface treatment

Length (μm)	Width (μm)	Measured frequency (MHz)	λ_T/h	$Q_{support}$	Q_{TED}	$Q_{analytical}$	$Q_{measured}$
700	8.7	0.74	315	17365	13768	7660	8000
500	6.1	1.03	227	18357	17142	8864	10700
500	7.2	1.21	193	11177	19476	7102	8300

crystal silicon C–C beam resonators with surface treatment is shown in Table 6. Our model overestimates the support loss in this case. This difference may be attributed to the ratio of λ_T/h not being large enough to validate the 2D assumption in the support region. As emphasized throughout the paper, our 2D analytical model is valid only under the condition that the transverse wavelength is much larger than the beam thickness. For a beam resonator with a small ratio of λ_T/h, 3D geometry should be included in the analytical model to predict support loss.

7. Conclusion

Support loss in micromachined beam resonators has been modeled based on the well-established theories of resonant beams and 2D elastic waves. Using the Fourier transform, closed-form expressions for the support quality factor are obtained, enabling performance trade-off for specific applications of beam resonators. This analytical model is applicable to both C–C and C–F micromachined beam resonators with in-plane flexural vibration and very large ratio of transverse wavelength to beam thickness (λ_T/h). The validity of this model has been demonstrated through comparison with experimental data. Further study on support loss in 3D geometry will overcome the application limit of this 2D analytical model.

Acknowledgements

This work is funded by DARPA NMASP program under contract # DAAH01-01-1-R004.

References

[1] G. Stemme, Resonant Silicon Sensors, J. Micromech. Microeng. 1 (1991) 113–125.
[2] H.A.C. Tilmans, M. Elwebspoek, J.H.J. Fluitman, Micro resonant force gauges, Sens. Actuators A 30 (1992) 35–53.
[3] S.P. Beeby, M.J. Tudor, Modelling and optimization of micromachined silicon resonators, J. Micromech. Microeng. 5 (1995) 103–105.
[4] J. Yang, T. Ono, M. Esashi, Energy dissipation in submicrometer thick single-crystal silicon cantilevers, J. Microelectromech. Syst. 11 (6) (2002) 775–783.
[5] S.Y. No, A. Hashimura, S. Pourkamali, F. Ayazi, Single-Crystal Silicon HARPSS Capacitive Resonators with Submicron Gap-Spacing, Tech. Dig. Solid-State Sensors, Actuators, and Microsystems Workshop, Hilton Head, SC, June 2002, pp. 281–284.
[6] K. Wang, A.-C. Wong, C.T.-C. Nguyen, VHF free–free beam high-Q micromechnical resonators, J. Microelectromech. Syst. 9 (3) (2000) 347–360.

[7] W.T. Hsu, J.R. Clark, C.T.C. Nguyen, Mechanically Temperature-Compensated Flexural-Mode Micromechanical Resonators Technical Digest, IEEE International Electron Deevices Meeting, vol. 11–13, San Francisco, California, 2000, pp. 399–402.
[8] C.T.C. Nguyen, Frequency-selective MEMS for miniaturized communication devices, in: Proceedings of the IEEE Aerospace Conference 1, Snowmass, Colorado, 21–28 March 1998, pp. 445–460.
[9] V.T. Srikar, S.D. Senturia, Thermoelastic damping in fine-grained polysilicon flexural beam resonators, J. Microelectromech. Syst. 11 (5) (2002) 499–504.
[10] B.H. Houston, D.M. Photiadis, M.H. Marcus, J.A. Bucaro, X. Liu, J.F. Vignola, Thermoelastic loss in microscale oscillators, Appl. Phys. Lett. 80 (7) (2002) 1300–1302.
[11] R. Liftshitz, M.L. Roukes, Thermoelastic damping in micro and nanomechanical systems, Phys. Rev. B 61 (8) (2000) 5600–5609.
[12] R. Lifshitz, M.L. Roukes, Thermoelastic damping in micro- and nanomechanical systems, Phys. Rev. B 61 (2000) 5600–5609.
[13] S. Pourkamali, A. Hashimura, R. Abdolvand, G.K. Ho, A. Erbil, F. Ayazi, High-Q single crystal silicon HARPSS capacitive beam resonators with self-aligned sub-100 nm transduction gaps, J. Microelectromech. Syst. 12 (2003) 487–496.
[14] K.Y. Yasumura, T.D. Stowe, E.M. Chow, T. Pfafman, T.W. Kenny, B.C. Stipe, D. Rugar, Quality factors in micron- and submicron-thick cantilevers, J. Microelectromech. Syst. 9 (1) (2000) 117–125.
[15] J. Yang, T. Ono, M. Esashi, Mechanical behavior of ultrathin microcantilever, Sens. Actuators A 82 (2000) 102–107.
[16] Y. Jimbo, K. Itao, Energy loss of a cantilever vibrator, J. Horolog. Inst. Jpn. 47 (1968) 1–15 (in Japanese).
[17] M.C. Cross, R. Lifshitz, Elastic wave transmission at an abrupt junction in a thin plate with application to heat transport and vibrations in mesoscopic systems, Phys. Rev. B 64 (2001) 1–22.
[18] L.D. Landau, E.M. Lifshitz, Theory of Elasticity, Pergamon Press, Oxford, 1959.
[19] P.M. Morse, Vibration and Sound, McGraw-Hill, New York, 1948.
[20] G.F. Miller, H. Pursey, The field and radiation impedance of mechanical radiators on the free surface of a semi-infinite isotropic solid, Proc. R. Soc. Lond. 223 (1954) 521–541.
[21] J.P. Gorman, Finite Element Model of Thermoelastic Damping in MEMS, Master Thesis, Materials Science and Engineering, Massachusetts Institute of Technology, June 2002.
[22] S.Y. No, A. Hashimura, S. Pourkamali, F. Ayazi, Single-Crystal Silicon HARPSS Capacitive Resonators with Submicron Gap-Spacing, Technical Digest Solid-State Sensors, Actuators, and Microsystems Workshop, Hilton Head, SC, June 2002, pp. 281–284.

Biographies

Zhili Hao received the BS and MS degrees in Mechanical Department from Shanghai JiaoTong University, Shanghai, PR China, in 1994 and 1997, respectively. She received her PhD degree from the University of Central Florida, Department of Mechanical, Materials and Aerospace Engineering, in 2000. The PhD project was the research and development of MEMS-based cooling system of microelecronics. From 2001 and 2002, Dr. Hao worked as a MEME Engineer with Nanovation Technologies, Inc., Northville, MI, and MEMS Optical, Inc., Huntsville, AL. She was involved in the development of various MEMS products, including tilt mirrors for telecom and projection display application, membrane and piston-type mirrors for adaptive optics application, microfluidic devices for biomedical and cooling application. She is currently a postdoctoral fellow with School of Electrical and Computer Engineering, Georgia Institute of Technology. Her research interests are in the development of RF MEMS devices and studying fundamental physical mechanisms in MEMS resonant devices, such as support loss and thermoelasitc damping.

Ahmet Erbil received his PhD in Physics from Massachusetts Institute of Technology in 1983. After 2 years at IBM Thomas J. Watson Research Center, he joined Georgia Tech Faculty to establish a program on electronic and photonic materials. He has been a Slona Research Fellow and a recipient of IBM Faculty Development Award. He was a visiting professor at Ecole Polytechnique Federale de Lausanne in Switzerland in the Fall of 1991. He has been consultant to several large industrial firms. He has also been principal investigator on more than 20 projects sponsored by government agencies and corporations. He holds five patents in the field of MOCVD chemicals and thin film production.

Farrokh Ayazi was born on 19 February 1972. He received the BS degree in electrical engineering from the University of Tehran, Iran, in 1994, and the MS and the PhD degrees in electrical engineering form the University of Michigan, Ann Arbor, in 1997 and 2000, respectively. He joined the faculty of Georgia Institute of Technology in December 1999, where he is currently as assistant professor in the School of Electrical and Computer Engineering. Prof. Ayazi's current research interests are in the areas of integrated MEMS, RF MEMS, analog VLSI, integrated microsystems, MEMS inertial sensors, and microfabrication technologies. Prof. Ayazi is the recipient of the Georgia Tech College of Engineering Cutting Edge Research Award for 2001–2002. He received a Rackham Predoctoral Fellowship from the University of Michigan for 1998–1999.